A MOLECULAR DYNAMICS SIMULATION STUDY ON THE INVESTIGATION OF THE MELTING PROCESS OF PURE ALUMINIUM USING DIFFERENT POTENTIALS

Murat Celtek[1*] , Unal Domekeli[2]

[1]*Faculty of Education, Trakya University, 22030, Edirne – TÜRKİYE*
[2]*Dept. of Physics, Trakya University, 22030, Edirne – TÜRKİYE*

* Corresponding author: mceltek@trakya.edu.tr

Abstract

In this study, the melting process of pure aluminum (Al) element has been investigated by molecular dynamics (MD) simulations using different interatomic potentials. Embedded atom method (EAM) potential, Sutton-Chen (SC) and tight-binding (TB) many-body potentials are used to describe the interactions between Al atoms. Atomic simulations have been performed with the classical MD simulation software DL_POLY 2.0 package program developed at Daresbury Laboratory. The process is explained using volume-temperature (V-T), potential energy-temperature (PE-T) curves, pair distribution function (PDF) and Honeycutt-Andersen (HA) pair analysis method. It has been observed that the selected potentials are generally successful, although they have differences in explaining the values such as the lattice parameter and cohesive energy of Al at low temperatures. On the other hand, it has been observed that all potentials predicted the melting point of Al at different points. Moreover, the results of the present study are discussed by comparing them with appropriate experimental results in the literature. We believe that the results will shed light on scientists planning to study Al and its alloys.

Keywords: aluminum, interatomic potential, melting point, molecular dynamic simulations, pair distribution functions.

INTRODUCTION

In recent years, thanks to the developments in technology and software, there have been positive developments in terms of speed and accuracy in molecular dynamics simulation techniques. Thanks to MD simulation, it is possible to access a lot of information about materials that is difficult to obtain under experimental conditions. Moreover, thanks to atomic simulations, it is now possible to understand the properties of materials under different conditions such as pressure, tension and temperature at the atomic level [1–3]. One of the most important criteria for the success of the MD simulation method is the most accurate explanation of the repulsive and attractive interaction forces between atoms. The way to achieve this is to choose the most appropriate interatomic potential function that can accurately describe the interactions within the system. Thus, in this study, we aimed to investigate the effect of different interatomic potentials on the melting process.

In the current study, we focused on the melting process of the aluminum (Al) element, which has many areas of use such as transportation, architecture, industrial areas, aviation, construction sector, electrical and electronics sector [4–6]. The melting process of this valuable element has been investigated using embedded atom method ((EAM1 [7] and EAM2 [8])) potential, Sutton-Chen (SC) [9] and tight-binding (TB) [10] many-body potentials.

EXPOSITION

All atomic simulations were performed using the DL POLY 2.0 package [11]. During the heating process, solid-liquid phase transitions were followed using the NPT isothermal isobaric ensemble at 0 GPa

pressure. During the simulations, pressure and temperature were controlled by Berendsen barostat and thermostat, respectively. Initially, Al atoms were placed at superlattice points to form face-centered cubic (fcc) crystal cells. The number of atoms in the MD simulation cell was determined to be 15x15x15x4=13,500. Periodic boundary conditions were applied along the x-, y- and z-directions of the simulation cell. In order to solve the Newton equations of motion, the velocity form of the Leapfrog Verlet algorithm and 2 fs as the time step were adopted. In order to initially remove the stress on the system, the system was first heated to 300 K and then cooled to 0 K. The system was then heated in $\Delta T = 50$ K steps up to 2500 K, which is sufficiently higher than the experimental melting point (T_m=933.5 K [12]) of Al. Moreover, in order to determine the first order solid-liquid phase transitions more accurately, the melting point of the system was studied with $\Delta T = 10$ K steps. A heating rate of 5 K/ps has adopted in all simulations.

The heating, solid-liquid phase transition process and liquid structure properties of Al element have been investigated using four different potentials. In our present study, two different embedded atom potential (EAM1 [7] and EAM2 [8]) data, Sutton-Chen (SC) [9] and tight-binding (TB) [10] many-body potentials, were used to explain the interactions between Al atoms.

According to the EAM model, the total energy resulting from interatomic interactions in a system of N atoms is defined as follows;

$$E_T = \frac{1}{2} \sum_{i,j,i\neq j}^{N} \varphi_{ij}(r_{ij}) + \sum_{i}^{N} F_i(\rho_i) \quad (1)$$

The first term here, $\varphi_{ij}(r_{ij})$ is the pair interaction energy, which represents the repulsive interactions between two bodies. The second term F_i is the embedding energy, which depends on the charge density ρ_i, which includes attractive interactions.

$$\rho_i = \sum_{j,j\neq i} f_j(r_{ij}) \quad (2)$$

Here $f_j(r_{ij})$ is the atomic charge density function.

SC potentials are also defined as long-range many-body EAM potentials of the Finnis–Sinclair [13] type and its analytical form is as follows;

$$E_T = \sum_i \left[\sum_{j(i\neq j)} \varepsilon_{ij} \frac{1}{2} V(r_{ij}) - C_i \varepsilon_{ij} (\rho_i)^{1/2} \right] \quad (3)$$

where $V(r_{ij})$ represents the pair potential and its form is as follows;

$$V(r_{ij}) = \left(\frac{a_{ij}}{r_{ij}} \right)^{n_{ij}} \quad (4)$$

The local density function ρ_i in equation 3 is defined as follows;

$$\rho_i = \sum_{j(i\neq j)} \phi(r_{ij}) \quad (5)$$

$$\phi(r_{ij}) = \left(\frac{a_{ij}}{r_{ij}} \right)^{m_{ij}} \quad (6)$$

Here r_{ij} is the distance between atoms i and j, a_{ij} is a parameter with dimension of length, C_i is a dimensionless parameter obtained by scaling the attractive term to the repulsive term, ε_{ij} is a parameter with dimension of energy, and n and m (n>m) are integer parameters providing elastic stability [14].

The form of the TB potential, similar to the EAM method, consists of two parts, attractive and repulsive, and its form is given as follows [10,15,16];

$$E_T = -\left\{ \sum_{j\neq i} \xi^2 exp\left[-2q\left(\frac{r_{ij}}{r_0} - 1 \right) \right] \right\}^{1/2} + \sum_{j\neq i} A\, exp\left[-p\left(\frac{r_{ij}}{r_0} - 1 \right) \right] \quad (7)$$

The first part has the same role as the embedding energy function $F_i(\rho_i)$ in the EAM method, that is, it is responsible for the attractive interactions in the system. The second part is responsible for the repulsive interactions in the system and has the Born-Mayer ion-ion pair potential type.

The cohesive energy (E_c(eV/atom)) , lattice parameter (a(Å)), melting temperature (T_m(K)), linear thermal expansion coefficient (ε(K^{-1})), heat capacity (C_p(J.mol^{-1}.K^{-1})) and density (ρ(g/cm^3)) values obtained for each potential are given in Table 1 together with the appropriate experimental results. The present findings show that EAM1 and TB potentials are more successful than others in predicting the relevant physical properties of Al. Moreover, the potential of EAM1 is one-step ahead of TB. These results reveal how important the selection of potential is in order to obtain reliable results for Al from MD simulations. Considering the large differences between the experimental conditions and the MD simulation conditions, it can be said that the results produced by the other potentials are also reasonable.

Table 1. *Some physical properties calculated for pure Al with four different potentials and their appropriate experimental data in the literature.*

	EAM1	EAM2	SC	TB	Exp.
E_c(eV/atom)	-3.36	-3.58	-3.35	-3.34	-3.39[a]
a(Å)	4.05	4.12	4.10	4.08	4.05[a]
T_m(K)	900	740	540	1140	933,5[a]
ε(x10^{-6}, K^{-1})	27.08	52.45	46.90	23.22	22.87[b]
C_p(J.mol^{-1}.K^{-1})	26.43	28.35	26.40	25.67	24.2[b]
ρ(g/cm^3)	2.70	2.57	2.59	2.65	2.70[c]

[a][12], [b][17], [c][18]

Fig. 1 depicts the temperature-dependent change of the volume per atom of pure Al heated using four different potentials. The first striking point in the figure is that while the volume per atom values obtained for EAM2, SC and TB potentials are close to each other at very low temperatures (T<200 K), it is seen that especially the TB potential results differ from the others with increasing temperature. While EAM1 produces larger volume values at low temperatures compared to other potentials, it produces values close to each other with TB as it approaches the melting point. Moreover, the EAM1, EAM2, SC and TB

potentials predict the melting point of Al as 900 K, 740 K, 540 K and 1140 K, respectively. Their deviations from the experimental melting point of Al are -3.59%, -20.72%, -42.15% and +22.12%, respectively. The present results show that the EAM1 potential predicts the melting point of Al closer to the experimental results than the others.
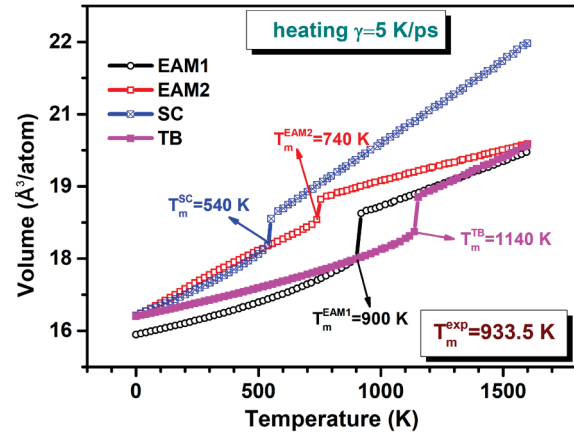

Fig. 1. *Volume per atom curves produced by different potentials during the heating process for pure Al.*

The variation of the potential energy per (PE-T) atom obtained for four potentials with respect to temperature is shown in Fig. 2. During the heating process, the PE-V curves obtained for all potentials show an almost linear increase up to the respective melting points. This means that there is no solid-solid or solid-liquid phase transition in the relevant temperature range. The sudden and sharp change in the PE-T curves corresponding to different temperature points for each potential with increasing temperature indicates that a first-degree solid-liquid phase transition occurs in the system. With further increase in temperature, the PE-T curves continue to increase almost linearly, indicating that the system is stable in liquid form.

In order to correctly perform structural analysis of the system in MD simulations, it is important to be able to predict well the characteristics of the central atom and what is happening around it, and moreover, the distance between them and other atoms. One of the simplest and most accurate ways

to do this is to calculate the pair distribution function (PDF or g(r)), which is one of the most preferred analyses. For more detailed information about the PDF, please see Ref [19].
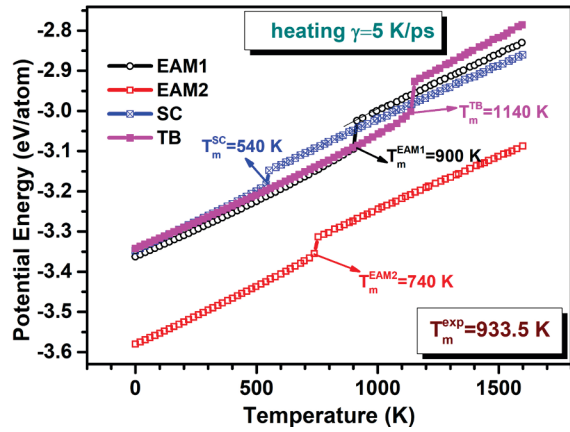

Fig. 2. Potential energy-temperature change for different potentials during the heating process.

The g(r) curves calculated around the melting point for the four potentials are presented in Fig. 3 together with the experimental liquid g(r) curves from the literature. We would like to note here that since the TB potential could not melt the system at 943 K, in order to compare the results, only the liquid data obtained at 940 K by cooling the system to liquid state with the TB potential was used for comparison. In general, it is seen that all potentials correctly predict the positions of the first and other peaks of the g(r) curves. It is seen that the peak heights and depths of g(r) for the SC and EAM2 potentials are slightly different from the experimental data. Supporting the results discussed above, the EAM1 and TB potential results are seen to be in excellent agreement with the experimental results. This is an indication that EAM1 and TB potentials are quite successful in predicting the properties of Al at both low and high temperatures.
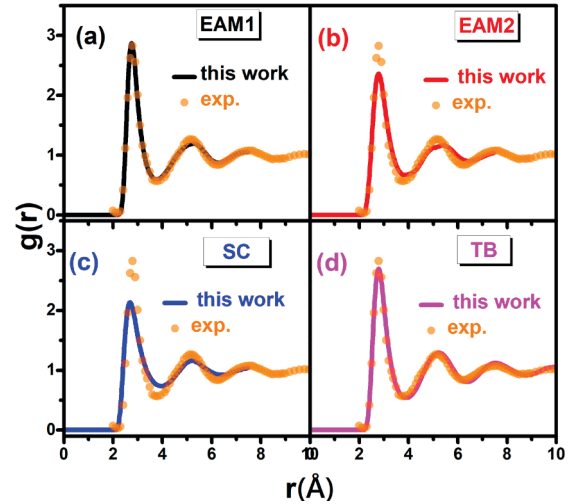

Fig. 3. Comparison of g(r) curves obtained for liquid Al using (a) EAM1, (b) EAM2, (c) SC and (d) TB potentials (940 K) with experimental data (943 K) [20].

PDF curves provide some information about the atomic structure of the system, but in order to better understand the micro world of the system, analysis methods such as Honeycutt-Andersen (HA) [21] are needed. With the HA method, it is possible to statistically examine the bonds that neighboring atoms in the system make with each other, the angles between them and the positions of the atoms. According to this method, 1551 bonded pairs represent ideal icosahedra, 1541 and 1431 pairs represent distorted icosahedra arrangement. 1421 bonded pairs represent fcc, 1422 bonded pairs represent close-packed hexagonal (hcp), and 1661 and 1441 bonded pairs represent body-centered (bcc) cubic crystal structures. More detailed information on HA can be found in Ref [22]. Some of the most common bonded pairs in the present study are shown schematically in Fig. 4.
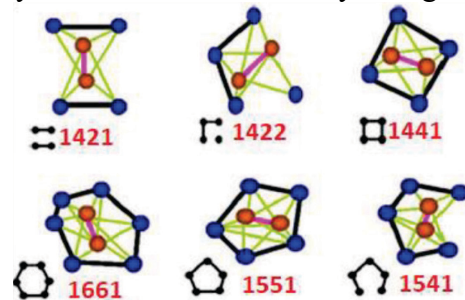
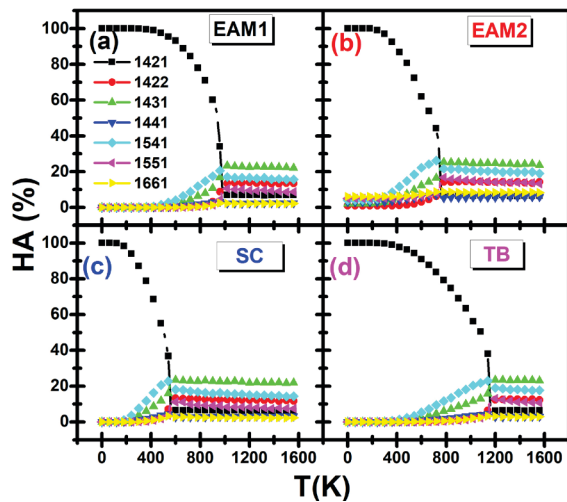

Fig.4. Some popular HA indices [23].

Fig.5. *Evolution of the most popular HA indices for (a) EAM1, (b) EAM2, (c) SC and (d) TB potentials during the heating process.*

Fig.5 shows the temperature dependent changes of HA analysis results for four potentials. The point that stands out in the figures is that although the potentials predict different melting points, they produce very similar results in terms of HA analyses. It can be seen from the figures that the distribution of 1421 bonded pairs representing the fcc structure at low temperatures is around 100% for each potential. This shows that each potential preserves the ideal fcc crystal structure, which is the initial structure of the system at low temperatures. While the number of 1421 bonded pairs decreases with increasing temperature, there is a slight increase in the number of 1431 and 1541 bonded pairs, which are especially common in amorphous and liquid structures. This means that the ideal fcc structure begins to deteriorate with increasing temperature and clusters of different structures begin to form within the system. Apart from these, there is no significant change in the number of other bonded pairs below the melting point, while their number appears to increase slightly after the melting point. The HA analysis results are consistent with the other results discussed above. No changes attributable to the solid-solid phase transition have been observed in the HA bonded pairs up to the melting point. The results have revealed the importance of the selection of potential functions for MD simulation studies.

CONCLUSION

In the present study, the heating process of pure Al element having fcc crystal lattice has been investigated by MD simulation method using EAM (EAM1 and EAM2), SC and TB many-body potentials. Although the physical and structural properties calculated from MD simulations at low and high temperatures using four potentials for pure Al are largely consistent with the experimental results in the literature, it was observed that EAM1 and TB potentials produced more consistent results than the others. Moreover, the melting temperature predicted by each potential for Al is different from each other. These are EAM1, EAM2, TB and SC potentials, respectively, according to their closeness to the experimental result. While the peak positions of the g(r) curves calculated from the EAM-MD results for four potentials, especially around the melting point, are consistent with the experimental data, their peak heights are in good agreement with the experimental ones only for the EAM1 and TB potentials. The results obtained from the HA method showed that the number of 1421 clusters representing the fcc crystal structure decreased with increasing temperature, while the number of clusters found in liquid and amorphous structures such as 1431 and 1541 increased. The results obtained as a result of this study showed that EAM1 and TB potential for pure Al element gave more successful and reliable results compared to others. It is believed that the results of the present study will guide the shaping of MD simulation studies on Al-containing alloys.

REFERENCE

[1] Cui Z, Zhang Y, Hu D, Vollebregt S, Fan J, Fan X, et al. Effects of temperature and grain size on diffusivity of aluminium: electromigration experiment and molecular dynamic simulation. Journal of Physics: Condensed Matter. 2022;34(17):175401.

[2] Celtek M. Atomic structure of Cu60Ti20Zr20 metallic glass under high pressures. Intermetallics. 2022;143.

[3] Guder V, Sengul S, Celtek M, Domekeli U. Pressure dependent evolution of microstructures in Pd80Si20 bulk metallic glass. Journal of Non-Crystalline Solids. 2022;576:121290.

[4] Starke EA, Staley JT. Application of modern aluminum alloys to aircraft. Progress in Aerospace Sciences. 1996;32(2–3):131–72.

[5] Schmidtke K, Palm F, Hawkins A, Emmelmann C. Process and Mechanical Properties: Applicability of a Scandium modified Al-alloy for Laser Additive Manufacturing. Physics Procedia. 2011;12:369–74.

[6] Domekeli U. A molecular dynamic study of the effects of high pressure on the structure formation of liquid metallic Ti62Cu38 alloy during rapid solidification. Computational Materials Science. 2021;187:110089.

[7] Sheng HW. EAM potentials [Internet]. 2021.

[8] Zhou XW, Johnson RA, Wadley HNG. Misfit-energy-increasing dislocations in vapor-deposited CoFe/NiFe multilayers. Physical Review B. 2004;69(14):144113.

[9] Sutton AP, Chen J. Long-range Finnis–Sinclair potentials. Philosophical Magazine Letters. 1990;61(3):139–46.

[10] Cleri F, Rosato V. Tight-binding potentials for transition metals and alloys. Physical Review B. 1993;48(1):22–33.

[11] Smith W, Forester TR. DL_POLY_2.0: A general-purpose parallel molecular dynamics simulation package. Journal of Molecular Graphics. 1996;14(3):136–41.

[12] Kittel C. Introduction to Solid State Physics. New York: John Wiley & Sons Inc.; 1986.

[13] Finnis MW, Sinclair JE. A simple empirical N-body potential for transition metals. Philosophical Magazine A. 1984;50(1):45–55.

[14] Domekeli U, Sengul S, Celtek M, Canan C. The melting mechanism in binary Pd 0.25 Ni 0.75 nanoparticles: molecular dynamics simulations. Philosophical Magazine. 2018;98(5):371–87.

[15] Celtek M, Sengul S, Domekeli U, Guder V. Dynamical and structural properties of metallic liquid and glass Zr48Cu36Ag8Al8 alloy studied by molecular dynamics simulation. Journal of Non-Crystalline Solids. 2021;566:120890.

[16] Celtek M. An in-depth investigation of the microstructural evolution and dynamic properties of Zr77Rh23 metallic liquids and glasses: a molecular dynamics simulation study. Journal of Applied Physics. 2022;132(3).

[17] Alüminyum. Vikipedi. 2024;https://tr.wikipedia.org/wiki/Alüminyum.

[18] Arblaster JW. Selected Values of the Crystallographic Properties of Elements. Materials Park, Ohio: ASM International.; 2018.

[19] Celtek M. The effect of atomic concentration on the structural evolution of Zr100-xCox alloys during rapid solidification process. Journal of Non-Crystalline Solids. 2019;513:84–96.

[20] Waseda Y. The Structure of Non-Crystalline Materials-Liquids and Amorphous Solids. New York: London: McGraw-Hill; 1981.

[21] Honeycutt JD, Andersen HC. Molecular Dynamics Study of Melting and Freezing of Small Lennard- Jones Clusters. Journal of Physical Chemistry. 1987;91(24):4950–63.

[22] Celtek M, Sengul S, Domekeli U, Guder V. Molecular dynamics simulations of glass formation, structural evolution and diffusivity of the Pd-Si alloys during the rapid solidification process. Journal of Molecular Liquids. 2023;372:121163.

[23] Celik FA, Korkmaz ET. Molecular dynamic investigation of the effect of atomic polyhedrons on crystallization mechanism for Cu-based Cu-Pd and Cu-Pt alloys. Journal of Molecular Liquids. 2020;314:113636.